Computational and Theoretical Chemistry 1081 (2016) 38–43

Contents lists available at ScienceDirect

Computational and Theoretical Chemistry

journal homepage: www.elsevier.com/locate/comptc

Reactive scattering of an electronically-excited nitrogen atom with H_2 and its isotopic variants: $N(^2D) + H_2/D_2/T_2$

Emine Tanis

Ahi Evran University, Kaman Vocational School, 40300 Kirsehir, Turkey

ARTICLE INFO

Article history:
Received 11 August 2015
Received in revised form 22 January 2016
Accepted 11 February 2016
Available online 20 February 2016

Keywords:
Reaction kinetics
Isotope effect
Centrifugal sudden approximation

ABSTRACT

Total reaction probabilities, integral cross sections and total rate constants of the $N(^2D) + H_2$ reaction and its isotopic variants were calculated using a time-dependent quantum wave packet method with a centrifugal sudden approximation on the latest reported global potential energy surface. The effect of rotational excitation of the diatoms and its projection quantum number on the behaviour of reaction probabilities was studied. Reaction probabilities were calculated using a flux wave packet method. The results indicate that the reaction kinetics are affected by intermolecular isotope and collision energies.

1. Introduction

Ground-state nitrogen $N(^4S)$ is inertial, and therefore, has a long lifetime and it is only slightly reactive (for symmetry and thermodynamical reasons). However, the title reaction of the first excited (^2D) state of nitrogen, $N(^2D) + H_2 \rightarrow NH(^3\sum^-) + H$, makes the excited nitrogen atom very reactive. Therefore, excited nitrogen plays a significant role in the chemistry of planetary atmospheres, combustion chemistry, interstellar chemistry and plasma chemistry [1]. Due to the reactive behaviour of the excited-state of the $N(^2D)$ atom, significant attention has been directed towards the atom in this state and its collisions with H_2 in recent experimental and theoretical studies [2–7]. The atmosphere of Saturn's largest moon, Titan, is mainly composed of molecular nitrogen, in addition to 2–5% methane [8,9] and some reaction products of $N(^2D)$ with simple hydrocarbons [10–12].

This chemical reaction has been studied both experimentally and theoretically [1–34]. The early experimental work of Fell et al. [13] monitored the concentrations of $N(^2D_{3/2})$ and $N(^2D_{5/2})$ with electron spin resonance. Afterwards, in 1991, Dodd et al. [14] studied vibrational distributions of NH and produced time-resolved infrared emission measurements. In another study, Suzuki et al. [15] obtained the temperature-dependent rate constants of the reactions of $N(^2D)$ with H_2 and D_2. Umemoto et al. [16–18] produced the excited nitrogen atom $N(^2D)$ by photodissociation of NO, and obtained the ratio of the vibrational levels of the NH molecule using an intense laser pulse at 275.2 nm in laser-induced fluorescence. In 1999, Alagia et al. [19] first performed a reactive scattering study of nitrogen atoms and obtained the angular and velocity distributions of the ND product from the reaction $N(^2D) + D_2$ using a crossed molecular beam. The obtained results were compared with early quasiclassical trajectory (QCT) calculations, which were theoretical, and the experimental and theoretical results were found to be similar. In 2001, Balucani et al. [20] performed further experimental and theoretical work. They obtained experimental values for the angular and velocity distributions of the ND product from crossed molecular beam experiments, and reproduced the centre-of-mass product angular and translational energy distributions. In the theoretical part of their study, the (QCT) method recently developed by Pederson et al. [21] was used.

Kobayashi and co-workers [22] theoretically developed an *ab initio* potential energy surface (PES) for the ground-state NH_2 system, based on first-order configuration interaction (FOCI) calculations. For $N(^2D) + H_2/D_2$ reactions, Pederson et al. [21] calculated reaction kinetics and product distributions on the ground (PES) by using (QCT) calculations based on the kernel Hilbert space interpolation method. They compared their results with calculations for the lower level of the first FOCI surface and found that the only true reaction path for their surface was the FOCI surface. Again, using this PES, Honvault and Launay [23] obtained reaction kinetics and product distributions using the hyperspherical coordinate quantum mechanical time-independent (QM-TI) method for total angular momentum quantum numbers, J, up to 26. Takayanagi and co-workers [24] computed two-dimensional PESs for the $N + H_2$ reaction using the *ab initio* multireference configuration interaction method. The calculations showed that not only the

http://dx.doi.org/10.1016/j.comptc.2016.02.010
2210-271X/

lowest doublet surface but also the second lowest doublet surface contributed to the reaction dynamics of $N(^2D) + H_2$. Rackham et al. [25] determined the exact quantum mechanical integral cross section with coupled channel capture theory and found that their result supported the results recently reported by Honvault Launay and the experimental evaluation of Umemoto et al. [17]. Ho et al. [26] calculated the differential cross sections (DCSs) and rate constants of the vibrational and rotational distributions of the $N(^2D) + H_2(X^1\sum_g^+)$ reaction on the ground-state PES, which they developed themselves. For the same PES, Banares and co-workers [27] calculated the integral cross sections and thermal rate constants for $N + H_2$ and its isotopic variants, which used the QCT method and statistical quantum-mechanical model methods. For the same PES, Castillo et al. [28] computed total initial state-selected and final state-resolved reaction probabilities and product rotational distributions for total angular momentum $J = 0$ using split operator and QCT methodologies. Due to the high reactivity of $N(^2D)$, Pederson and co-workers [29] presented a global PES for the second lowest electronic state ($1^2A'$) depending on an interpolation technique known as reproducing the kernel Hilbert space (RKHS), and Akpinar et al. [30] calculated the reaction dynamics of $N(^2D) + H_2$ using the QCT method on this PES. In addition to theoretical studies, several dynamical studies have also been recently reported [31–34].

Yang et al. [35] constructed a new analytical potential energy surface (APES) for the $N(^2D) + H_2(X^1\sum_g^+) \rightarrow NH(X^3\sum^-) + H(^2S)$ reaction. In this reaction, the N atom is in the excited [36] D state for the $N + H_2$ asymptote, but in the ground state for the NH + H asymptote; consequently, the same atom has different states in different dissociative asymptotes [35]. This new potential surface is represented with a many-body expansion and a new switch function that contains all of the interatomic distances of the system. It is accurate in the range of small internuclear distances, which can ensure reliable potential energies for each part of the dynamics structure [35].

In our study, the real wave packet (RWP) method was used to study $N + H_2(D_2/T_2)$ reactions, combined with a flux method and a centrifugal sudden (CS) approximation for $J > 0$ states. The rest of this paper is organised as follows. The theory is outlined in Section 2 and the results are discussed in Section 3.

2. Method

In the present study, the RWP method of Gray and Balint-Kurti [37] using the Chebyshev operator propagator method was used to calculate the reaction dynamics of $N(^2D) + H_2$ and its isotopic variants on the PES provided by Yang et al. [35]. To study $N(^2D) + H_2/D_2/T_2$, a body-fixed (BF) frame representation was adopted with reactant Jacobi coordinates [38], identified as $(R_\alpha, r_\alpha, \gamma_\alpha, K_\alpha)$. As in previous work [32], the Hamiltonian for $J = 0$ was expressed in the product Jacobi coordinates, $(R_\alpha, r_\alpha, \gamma_\alpha)$. Here R_α is the distance from the N atom to the centre of mass of the $H_2/D_2/T_2$ molecule, r is the vibrational coordinate of the diatomics and, γ is the angle between R and the r vectors [39].

In the reactant Jacobi coordinates$(R_\alpha, r_\alpha, \gamma_\alpha)$, the Hamiltonian for a given total angular momentum J can be written as

$$\widehat{H} = -\frac{\hbar^2}{2\mu_{R_\alpha}}\frac{\partial^2}{\partial R_\alpha^2} - \frac{\hbar^2}{2\mu_{r_\alpha}}\frac{\partial^2}{\partial^2 r_\alpha} + \frac{(J-j)^2}{2\mu_{R_\alpha}R_\alpha^2} + \frac{j^2}{2\mu_{r_\alpha}r_\alpha^2} + V(R_\alpha, r_\alpha, \gamma_\alpha) \quad (1)$$

where μ_{R_α} indicates the reduced masses of N and H_2 and, μ_{r_α} indicates the reduced mass of H_2. J is the total angular momentum operator, j is the rotational angular momentum operator of H_2 and $V(R_\alpha, r_\alpha, \gamma_\alpha)$ is the PES of the N–H_2 system described previously [35]. With a spherical harmonic basis, $y_{jK}(\theta_\alpha)$ is used for the angular degree of freedom, which as a finite basis representation (FBR) time-dependent wave packet can be given as [38,40–43].

$$\psi^{JM\varepsilon}(R_\alpha, r_\alpha, t) = \sum_{K_\alpha} D^{J\varepsilon^*}_{MK_\alpha}(\Omega_\alpha)\psi_\alpha(t, R_\alpha, r_\alpha, \theta_\alpha^{K_\alpha}; K_\alpha) \quad (2)$$

where $D^{J\varepsilon^*}_{MK_\alpha}(\Omega_\alpha)$ is the normalised rotation matrix

$$D^{J\varepsilon^*}_{MK_\alpha}(\Omega_\alpha) = (1+\delta_{K_\alpha 0})^{-1/2}\sqrt{\frac{2J+1}{8\pi}}\left[D^J_{MK_\alpha}(\Omega_\alpha) + \varepsilon(-1)^{J+K_\alpha}D^J_{M-K_\alpha}(\Omega_\alpha)\right] \quad (3)$$

Here $\varepsilon = (-1)^{l+j}$ is the parity, l is the orbital angular momentum quantum number and K is the projection of the total angular momentum J along the BF z-axis (R) [44]. In Eq. (2) $\psi_\alpha(t, R_\alpha, r_\alpha, \theta_\alpha^{K_\alpha}; \Omega_\alpha)$, which depends only on three internal coordinates of the system and the projection of the total angular momentum K_α on the BF z-axis can be written as

$$\psi_\alpha(t, R_\alpha, r_\alpha, \theta_\alpha^{K_\alpha}; K_\alpha) = \sum_{n,m,j} F^{K_\alpha}_{nmj}(t)u_n(R_\alpha)\phi_m(r_\alpha)y_{jK_\alpha}(\theta_\alpha) \quad (4)$$

Here n and m are the translational basis labels, $u_n(R_\alpha)$ and $\phi_m(r_\alpha)$ are the translational basis functions for R and r, respectively and $y_{jK_\alpha} = \sqrt{[(2j+1)/4\pi]}d^j_{K_\alpha 0}$ indicates the spherical harmonics. $d^j_{\Omega_\alpha\Omega_\nu}$ is a reduced Wigner rotational matrix [45] with $\Omega_\nu = 0$.

In Eq. (1), the Coriolis coupling term, which is off-diagonal in K states in the BF representation is given by

$$\frac{\hbar^2}{2\mu_r R^2}\left\langle Y^{JM\varepsilon}_{jK}|(J-j)^2|Y^{JM\varepsilon}_{j'K'}\right\rangle\delta_{nn'}\delta_{\nu\nu'} \quad (5)$$

$$= \frac{\hbar^2}{2\mu_r R^2}\delta_{jj'}\Big\{[J(J+1)+j(j+1)-2K^2]\delta_{KK'} - \lambda^+_{jK}\lambda^+_{jK}(1+\delta_{K0})^{1/2}$$
$$\delta_{K+1,K'} - \lambda^-_{jK}\lambda^-_{jK}(1+\delta_{K1})^{1/2}\delta_{K-1,K'}\Big\}$$

and the quantityλ is denoted as

$$\lambda^\pm_{JK} = \sqrt{J(J+1) - K(K\pm 1)} \quad (6)$$

$$\lambda^\pm_{jK} = \sqrt{j(j+1) - K(K\pm 1)} \quad (7)$$

Eqs. (6) and (7) define the so-called Coriolis coupling terms [46,47]. In these equations, different K states in the wave function couple together. For this reason, more basis functions are needed to store the exact information about the wave function. Increasing the number of grid points in the angular part requires more computer memory. Hence, here, for computing the reaction probabilities for $J > 0$, the (CS) approximation was used. In the CS approximation, these off-diagonal elements are ignored, which considerably decreases the size of the Hamiltonian matrix [48]

$$\widehat{H} = -\frac{\hbar^2}{2\mu_{R\alpha}}\frac{\partial^2}{\partial R_\alpha^2} - \frac{\hbar^2}{2\mu_{r_\alpha}}\frac{\partial^2}{\partial r_\alpha^2} + \frac{\hbar^2}{2}\left(\frac{1}{2\mu_{R\alpha}R_\alpha^2} + \frac{1}{2\mu_{r\alpha}r_\alpha^2}\right)j^2$$
$$+ \frac{1}{2\mu_{R\alpha}R_\alpha^2}\times\{J(J+1) - 2K^2\} + V(R_\alpha, r_\alpha, \gamma_\alpha) \quad (8)$$

The reactant wave packet is set up in the reactant Jacobi coordinates, $\psi(R_\alpha, r_\alpha, \gamma_\alpha, t)$, and is then transformed to the product Jacobi coordinates, $\psi(R_\beta, r_\beta, \gamma_\beta, t)$ [38]. The reactant wave function can be written as

$$\psi(R_\alpha, r_\alpha, \gamma_\alpha, t) = e^{-ik_0(R_\alpha - R_{0,\alpha})}e^{-\beta(R_\alpha - R_{0,\alpha})}$$
$$\times\frac{\sin[\alpha(R_\alpha - R_{0,\alpha})]}{R_\alpha - R_{0,\alpha}}\varphi_{v_j}(r_\alpha)P_j(\cos\gamma_\alpha) \quad (9)$$

where $\varphi_{v_j}(r_\alpha)$ indicates the vibrational components and $P_j(\cos\gamma_\alpha)$ indicates the rotational components of the wave function. The

$e^{-ik_0(R_\alpha - R_{0,\alpha})}$ component gives an initial momentum to the initial wave function. After the reactant wave packet is constructed, it can be propagated on the PES according to the following Chebyshev propagator [49,50]. The Chebyshev propagator is carried through the following modified Chebyshev recursion relation recommended by Mandelshtam and Taylor [51,52].

$$\varphi_{k+1} = D(2\hat{H}_s\varphi_k - D\varphi_{k-1}) \tag{10}$$

$$\text{with } \varphi_1 = DH_s\varphi_0 \text{ and } \varphi_0 = \psi^{JM\varepsilon}_{\alpha v_0 j_0 t_0}(t=0) \tag{11}$$

The scaled Hamiltonian is

$$\hat{H}_s = a_s\hat{H} + b_s \tag{12}$$

with $a_s = 2/(H_{\max} - H_{\min})$ and $b_s = 1 + a_s H_{\min}$. a_s and b_s are chosen such that the minimum and maximum eigenvalues of $\hat{H}_s$ lie in the interval $(-1,1)$. The damping function D is applied at the grid edges, as presented by Lin and Guo [53]. k is the iteration step, $k = 1,2,\ldots,N$. This recursion requires φ_0 and φ_1 to be initialized. φ_0 is taken as the real part of the initial wave packet, while φ_1 is calculated as

$$\varphi_1 = D\left[\hat{H}_s\varphi_0 - \sqrt{1-\hat{H}_s^2}p_0\right] \tag{13}$$

where p_0 is the imaginary part of the initial wave packet. The action of the $\sqrt{1-\hat{H}_s^2}$ operator on p_0 is calculated with a Chebyshev polynomial expansion [54].

In the RWP approach, the Hamiltonian operator is mapped as

$$f(\hat{H}) = -\frac{\hbar}{\tau}\cos^{-1}(\hat{H}_s) \tag{14}$$

RWP is improved under the modified time-dependent Schrödinger equation

$$i\hbar\frac{\partial\psi(R_\alpha, r_\alpha, \gamma_\alpha, t)}{\partial t} = f(\hat{H})\psi(R_\alpha, r_\alpha, \gamma_\alpha, t) \tag{15}$$

The total reaction probability and the total reaction cross sections are calculated using a flux analysis method. This method extracts the wave packet at the analysis line, r_d, where the flux analysis is carried out [55,56]. The reaction probability is given as

$$P_i^{JK}(E) = \frac{\hbar}{\mu_R}\mathrm{Im}\left[\left\langle\psi(R, r_d, \gamma, E)\middle|\frac{\partial\psi(R, r_d, \gamma, E)}{\partial r}\right\rangle\right] \tag{16}$$

The total reaction cross section is given by

$$\sigma_{v_0 j_0 k_0}(E) = \frac{\pi}{k^2}\sum_J (2J+1)P^J_{v_0 j_0 k_0}(E) \tag{17}$$

$$\sigma_{v_0 j_0 k_0}(E) = \frac{1}{2j_0+1}\sum_{k_0}\sigma_{v_0 j_0 k_0}(E) \tag{18}$$

where k is the wavenumber corresponding to the initial state at a fixed collision energy E. v_0, j_0 and k_0 (the projection quantum number of j_0) are the initial quantum numbers used to denote the initial rovibrational state. Finally, the rate constant is obtained from the total reaction cross section for a given initial rovibrational state [57]

$$k_{v_0 j_0}(T) = \sqrt{\frac{8k_BT}{\pi\mu_R}}(k_BT)^{-2}\int_0^\infty E\sigma_{v_0 j_0}(E)\exp\left(-\frac{E}{k_BT}\right)dE \tag{19}$$

where k_B is the Boltzmann constant.

3. Results and discussion

Total reaction probabilities as a function of collision energy for the $H_2/D_2/T_2$ reagent molecules, as well as for its $v = 0$, $j = 0$ ground state with different total angular momentum values ($J = 10$, $J = 20$, $J = 30$, $J = 40$), are shown in Fig. 1. As can be seen, all of the calculated $P(E_c)$ values, with $J = 10$, 20, 30, 40 show a threshold, and the larger the total angular momentum quantum numbers, the greater the reaction threshold energies with the same reactive system. This shifting to higher collision energies is a result of the centrifugal potential barrier increasing with an increase in J. The reaction probabilities rise sharply near the threshold at $J = 10$ and $J = 20$ for all reactions. However, the reaction probabilities are not available for the $v = 0$, $j = 0$, $J = 30$ quantum state for the $N + H_2$ reaction. Therefore, the reaction probabilities are not available for the $v = 0$, $j = 0$, $J = 40$ quantum states for the H_2 and D_2 isotopes. This state is attributed to the mass of molecules. Hence, the effect of the total angular momentum quantum numbers ($J = 30$ and $J = 40$) on the centrifugal potential barrier is dominant over the mass of molecules. Similar behaviour was also observed in Zhang et al. [58], where a surface proposed by Zhai and Han [59] and Castillo et al. [28] was used, with the PES of Ho et al. [26].

The reaction probabilities of H_2 and its isotopic variants (D_2 and T_2) for different values of the projection quantum numbers $K = 0$ and 1 for $j = 1$ as a function of collision energy are shown in Fig. 2. The top and bottom panels of the figure represent $K = 0$ and $K = 1$, respectively. When the quantum number K increases, the reaction probabilities shift to lower energies. In particular, the reaction probabilities become more obvious when considering the isotope effect, i.e. the larger the molecular mass (T_2), the lower its threshold energy. When the quantum number K increases, this isotope effect becomes more pronounced.

The energy dependence of the integral reaction cross sections for the reactions of H_2 and its isotopes is demonstrated in Fig. 3. The cross sections show a threshold energy, which increases monotonically with energy. The calculations indicate that the convergence of the cross sections needs 30 or 40 partial waves for the $H_2/D_2/T_2$ reactions. Additionally, the isotope effect is seen to be less effective over the integral cross section. While the reaction probabilities in Fig. 1 have different threshold energies for isotope molecules, the integral cross sections for an averaged J show nearly the same threshold. These results support the outcome of a previous study by Chu et al. [2].

In order to investigate the rotational effect of the diatomic molecule on the dynamics properties of H_2 and its variants, integral cross sections with different rotational quantum numbers were calculated and are presented in Fig. 4. Our results are compared to the QCT results in Ref. [27] on the PES of Ho et al. [26] and exact WP results [4] obtained on the same PES. On the this PES [26], Lin and Guo [4] calculated the first exact ICSs and rate constants for the $N(^2D) + H_2(v = 0, j = 0, 2)$ reaction using a Chebyshev quantum close-coupling (CC) WP method. In this method, Coriolis coupling effect is taken into account. The figure shows that, all the results have a similar shape. Because of existence of barrier (Yang et al. PES ~ 0.99 meV – Ho et al. PES 0.84 meV) along the minimum energy path on the two PESs, threshold exists in all ICSs as showing in the figure. The threshold values of QCT (70–75 meV) and exact WP method results are smaller due to the lower energy barrier on our PES comparing with Ho PES. The results indicate that the reaction cross sections (ICS) enhanced by the rotational quantum numbers have nearly the same threshold energy. Moreover, the cross section increases monotonically with the energy for all reactions. It is emphasized that our results have smaller integral cross sections for the $N(^2D) + H_2(v = 0, j = 0, 1, 2)$ and $N(^2D) + D_2(v = 0, j = 0, 1, 2)$ reactions and less marked oscillations when compared with those of Refs. [27,4].

Rate constants for the $H_2/D_2/T_2$ molecules in the temperature range 300–500 K are presented in Fig. 5. The reaction rate

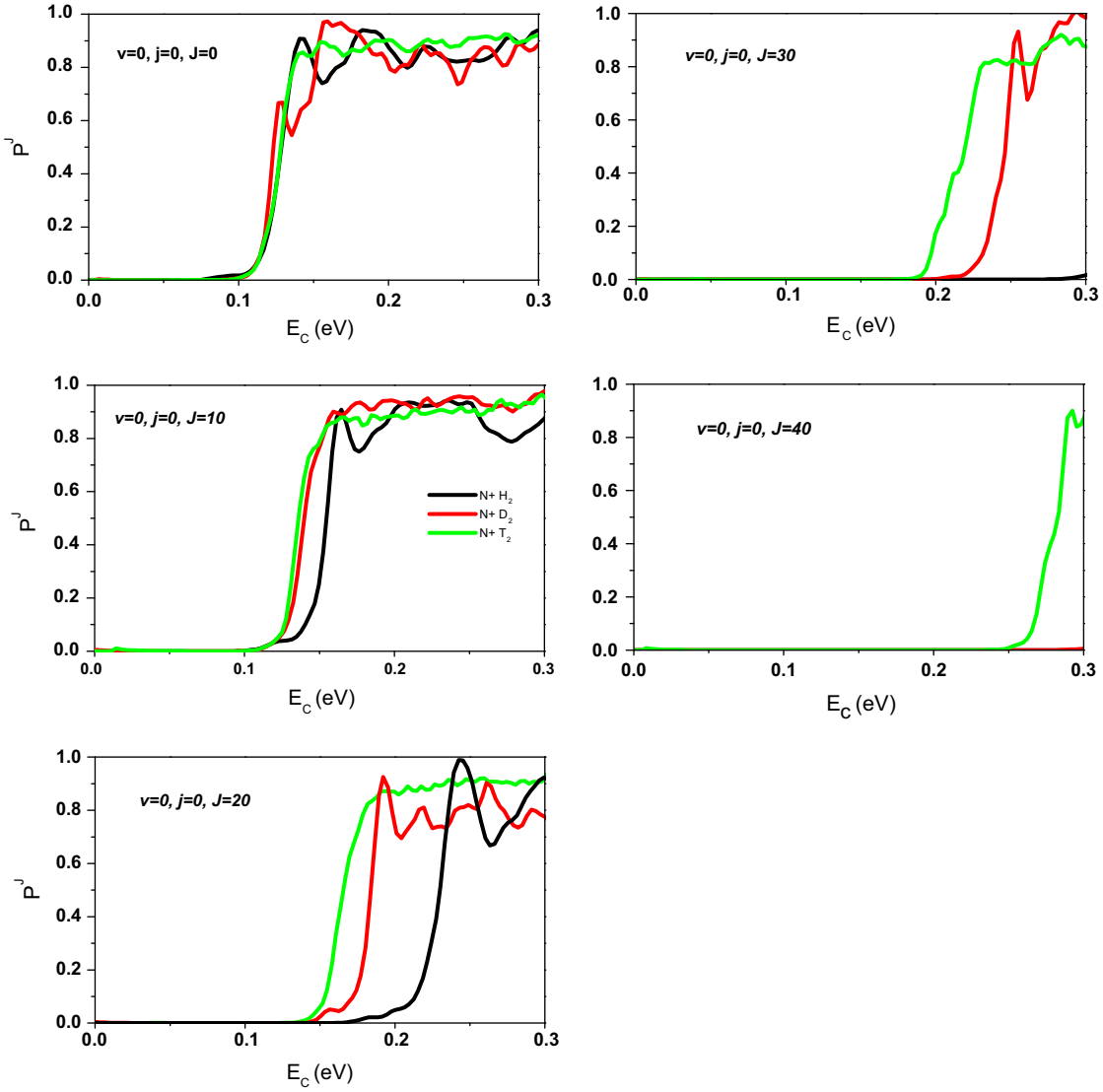

Fig. 1. Total reaction probabilities for the selected values of the total angular momentum quantum number J as a function of collision energy, ranging from 0 to 0.3 eV for H_2, D_2 and T_2, initially in their ground rovibrational state.

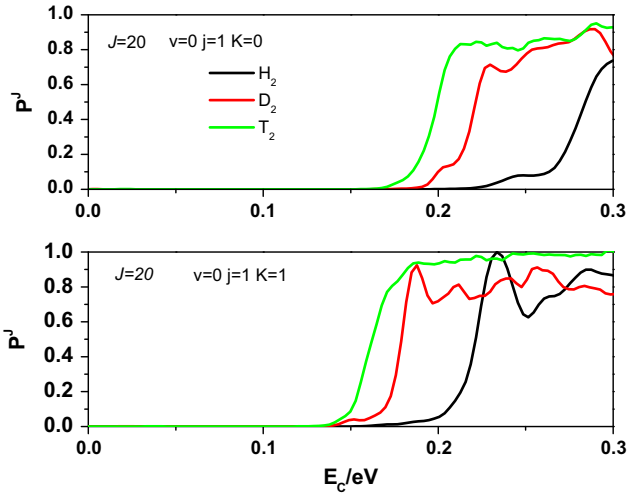

Fig. 2. Total reaction probabilities of H_2 and its isotopic variants (D_2 and T_2) for total angular momentum $J = 20$ with projection quantum number $K = 0$ and $K = 1$.

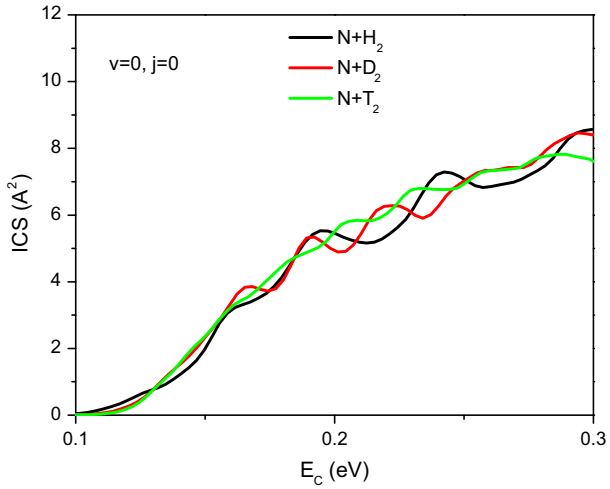

Fig. 3. Comparison between integral cross sections over the collision energy range of 0–0.3 eV for the reactions N + H_2/D_2/T_2.

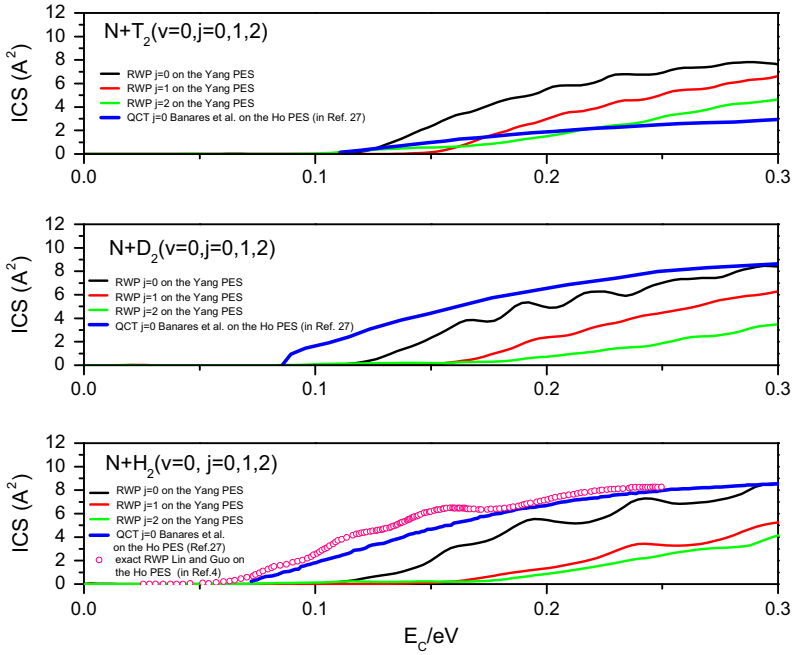

Fig. 4. Comparison between the RWP_Flux integral cross sections for $N(^2D) + H_2/D_2/T_2$ $(v = 0, j = 0, 1, 2)$ from the current calculations on the PES of Yang et al. [35] and previous calculations employing QCT integral cross sections on the PES of Ho et al. [26] and exact WP integral cross section [4] for $N(^2D) + H_2$ $(v = 0, j = 0, 1, 2)$ reaction on the same PES [26].

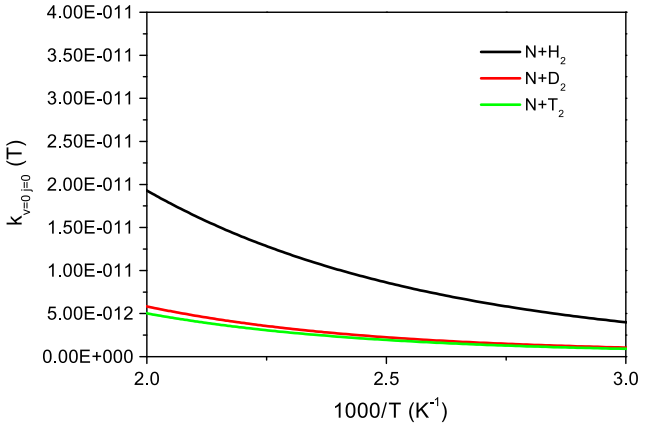

Fig. 5. Reaction rate constants as a function of temperature for $N(^2D) + H_2/D_2/T_2$ reactions.

constants decrease with decreasing temperature, which is compatible with exothermic reactions. The experimental [60] and theoretical [2] values were previously studied. However, to our knowledge, the current study is the first investigation in this range of temperatures.

4. Conclusions

In our study, state-selected reaction cross sections and reaction rate constants were calculated for the $N(^2D) + H_2$ reactive system and its isotopic variants on the excited state $(1^2A'')$ a new PES [35]. Besides this, the effect of several selected initial rotational states $(j = 0, 1, 2)$ of the initial molecules and projection quantum numbers (K) were investigated. This new PES results have been carefully compared with other PES [26] available in the literature. The results showed that the initial rotational quantum number of the initial molecule, its projection (K) and the isotope effect had a noticeable effect on the reaction dynamics. The reaction probabilities and cross sections displayed a threshold energy due to the centrifugal potential barrier. The calculated integral cross sections are somewhat agreement with the available theoretical results.

Acknowledgments

The author is grateful to Prof. Dr. Niyazi Bulut for providing computational support. This work was supported by Ahi Evran University – Turkey through a Project (PYO-FEN.4001.13.004). The numerical calculations were performed at TUBITAK ULAKBIM, High Performance and Grid Computing Center. The author is thankful to TUBITAK and Ahi Evran University BAP.

References

[1] P. Casavecchia, N. Balucani, M. Alagia, L. Cartechini, G.G. Volpi, Reactive scattering of oxygen and nitrogen atoms, Acc. Chem. Res. 32 (1999) 503.
[2] T.S. Chu, K.L. Han, A.J.C. Varandas, A quantum wave packet dynamics study of the $N(^2D) + H_2$ reaction, J. Phys. Chem. A 110 (2006) 1666–1671.
[3] N. Balucani, P. Casavecchia, L. Bañares, F.J. Aoiz, T. Gonzalez-Lezana, P. Honvault, J.M. Launay, Experimental and theoretical differential cross sections for the $N(^2D) + H_2$ reaction, J. Phys. Chem. A 110 (2006) 817–829.
[4] S.Y. Lin, H. Guo, Exact quantum dynamics of $N(^2D) + H_2 \rightarrow NH + H$ reaction: cross-sections, rate constants, and dependence on reactant rotation, J. Chem. Phys. 124 (2006) 031101.
[5] S.Y. Lin, L. Bañares, H. Guo, Differential and integral cross sections of the $N(^2D) + H_2 \rightarrow NH + H$ reaction from exact quantum and quasi-classical trajectory calculations, J. Phys. Chem. A 111 (2007) 2376–2384.
[6] B.J. Rao, S. Mahapatra, Quantum wave packet dynamics of $N(^2D) + H_2$ reaction, J. Chem. Phys. 127 (2007) 244307.
[7] X.F. Yue, J. Cheng, H. Li, Y.-Q. Zhang, E.L. Wu, Stereodynamics study of reactions $N(^2D) + HD \rightarrow NH + D$ and $ND + H$, Chin. Phys. B 19 (2010) 043401.
[8] H.B. Niemann, S.K. Atreya, J.E. Demick, et al., Composition of Titan's lower atmosphere and simple surface volatiles as measured by the Cassini–Huygens probe gas chromatograph mass spectrometer experiment, J. Geophys. Res. 115 (2010) E12006.
[9] R.V. Yelle, J. Cui, J. Muller-Wodarg, Methane escape from Titan's atmosphere, J. Geophys. Res. 113 (2008) E10003.
[10] (a) N. Balucani, L. Cartechini, M. Alagia, P. Casavecchia, G.G. Volpi, Observation of nitrogen-bearing organic molecules from reactions of nitrogen atoms with hydrocarbons: a crossed beam study of $N(^2D)$ + ethylene, J. Phys. Chem. A 104 (2000) 5655–5659;
(b) N. Balucani, M. Alagia, L. Cartechini, P. Casavecchia, G.G. Volpi, K. Sato, T. Takayanagi, Y. Kurosaki, Cyanomethylene formation from the reaction of

excited nitrogen atoms with acetylene: a crossed beam and ab initio study, J. Am. Chem. Soc. 122 (2000) 4443–4450.
[11] (a) H. Umemoto, T. Asai, H. Hashimoto, T. Nakae, Reactions of N(2^2D) with H_2O and D_2O; identification of the two exit channels, NH(ND) + OH(OD) and H(D) + HNO(DNO), J. Phys. Chem. A 103 (1999) 700–704;
(b) H. Umemoto, T. Nakae, H. Hashimoto, K. Kongo, M. Kawasaki, Reactions of N(2 D2) with methane and deuterated methanes, J. Chem. Phys. 109 (1998) 5844.
[12] (a) Y.L. Yung, An update of nitrile photochemistry on Titan, Icarus 72 (1987) 468–472;
(b) L.M. Lara, E. Lellouch, J.J. Lopez-Moreno, R. Rodrigo, Vertical distribution of Titan's atmospheric neutral constituents, J. Geophys. Res. 101 (1996) 23261.
[13] B. Fell, I.V. Rivas, D.L. McFadden, Kinetic study of electronically metastable nitrogen atoms, N(2 2DJ), by electron spin resonance absorption, J. Phys. Chem. 85 (1981) 224–228.
[14] J.A. Dodd, S.J. Lipson, D.J. Flanagan, W.A.M. Blumberg, NH ($X\ ^3\sum^-$, v = 1–3) formation and vibrational relaxation in electron-irradiated Ar/N_2/H_2 mixtures, J. Chem. Phys. 94 (1991) 4301.
[15] T. Suzuki, Y. Shihira, T. Dato, H. Umemoto, S. Tsunashima, Reactions of N(2^2D) and N(2^2P) with H_2 and D_2, J. Chem. Soc. Faraday Trans. 89 (1993) 995–999.
[16] H. Umemoto, M. Matsumoto, Production of NH(ND) radicals in the reactions of N(2^2D) with H_2(D_2): nascent vibrational distributions of NH($X\ ^3\Sigma^-$) and ND($X\ ^3\Sigma^-$), J. Chem. Phys. 104 (1996) 9640.
[17] H. Umemoto, T. Asai, Y. Kimura, Nascent rotational and vibrational-state distributions of NH(X (3)Sigma(-)) and Nd(X (3)Sigma(-)) Produced in the Reactions of N(2 D-2) with H-2 and D-2, J. Chem. Phys. 106 (1997) 49854991.
[18] H. Umemoto, Leaving-atom isotope effect in the reactions of N(2^2D) with isotopic hydrogens, Chem. Phys. Lett. 292 (1998) 594–600.
[19] M. Alagia, N. Balucani, L. Cartechini, P. Casavecchia, G.G. Volpi, L.A. Pederson, G. C. Schatz, G. Lendvay, L.B. Harding, T. Hollebeek, T.-S. Ho, H. Rabitz, Exploring the reaction dynamics of nitrogen atoms: a combined crossed beam and theoretical study of N(2D) + D2 → ND+D, J. Chem. Phys. 110 (1999) 8857.
[20] N. Balucani, M. Alagia, L. Cartechini, P. Casavecchia, G.G. Volpi, Dynamics of the N(^{2}D) + D_2 reaction from crossed-beam and quasiclassical trajectory studies, J. Phys. Chem. A 105 (2001) 2414.
[21] L.A. Pederson, G.C. Schatz, T.-S. Ho, T. Hollebeek, H. Rabitz, L.B. Harding, G. Lendvay, Potential energy surface and quasiclassical trajectory studies of the N (2D) + H2 reaction, J. Chem. Phys. 110 (1999) 9091.
[22] H. Kobayashi, T. Takayanagi, K. Yokoyama, T. Sato, S. Tsunashima, Quasiclassical trajectory studies of N(^{2}D) + H_2 reaction on a fitted *ab initio* potential-energy surface, J. Chem. Soc. Faraday Trans. 91 (1995) 3771–3777.
[23] P. Honvault, J.-M. Launay, A quantum-mechanical study of the dynamics of the N(^{2}D) + H_2 → NH + H reaction, J. Chem. Phys. 111 (1999) 6665–6667.
[24] T. Takayanagi, Y. Kurosaki, K. Yokoyama, Ab initio molecular orbital calculations of potential energy surfaces for the $N(^4S, ^2D, ^2P) + H_2$ reactions, Chem. Phys. Lett. 321 (2000) 106–112.
[25] E.J. Rackham, F. Huarte-Larranaga, D.E. Manolopoulos, Coupled-channel statistical theory of the $N(^2D) + H_2$ and $O(^1D) + H_2$ insertion reactions, Chem. Phys. Lett. 343 (2001) 356–364.
[26] T.S. Ho, H. Rabitz, F.J. Aoiz, L. Banares, S.A. Vázquez, L.B. Harding, Implementation of a fast analytic ground state potential energy surface for the $N(^2D) + H_2$ reaction, J. Chem. Phys. 119 (2003) 3063.
[27] L. Banares, F.J. Aoiz, T. Gonzalez-Lezana, V.J. Herrero, I. Tanarro, Influence of rotation and isotope effects on the dynamics of the $N(^2D) + H_2$ reactive system and of its deuterated variants, J. Chem. Phys. 123 (2005) 224301.
[28] J.F. Castillo, N. Bulut, L. Banares, F. Gogtas, Wave packet and quasiclassical trajectory calculations for the $N(^2D) + H_2$ reaction and its isotopic variants, Chem. Phys. 332 (2007) 119–131.
[29] L.A. Pederson, G.C. Schatz, T. Hollebeek, T.-S. Ho, H. Rabitz, L.B. Harding, Potential energy surface of the $\tilde{A}$ state of NH_2 and the role of excited states in the N(^{2}D) + H_2 reaction, J. Phys. Chem. A 104 (2000) 2301–2307.
[30] S. Akpinar, P. Defazio, P. Gamallo, C. Petrongolo, Quantum dynamics of NH($a^1\Delta$) + H reactions on the NH_2 $\tilde{A}^2A_1$ surface, J. Chem. Phys. 129 (2008) 174307.
[31] P. Gamallo, P. Defazio, M. Gonzalez, C. Petrongolo, Renner–teller coupled-channel dynamics of the $N(^2D) + H_2$ reaction and the role of the NH_2 $\tilde{A}^2A_1$ electronic state, J. Chem. Phys. 129 (2008) 244307.
[32] E. Karabulut, E. Aslan, N. Bulut, Quantum wave packet dynamics of the N(2D) + H2 reaction, Commun. Comput. Chem. 2 (2014) 21–36.
[33] E. Karabulut, E. Aslan, J. Kłos, N. Bulut, The effect of initial rotation in the N(^{2}D) + H_2 → NH($^3\Sigma^-$) + H reaction, Chem. Phys. 441 (2014) 53–58.
[34] M. Hankel, X.-F. Yue, Quantum dynamics study of the N(^{2}D) + H_2 reaction and the effects of the potential energy surface on the propagation time, Comp. Theor. Chem. 990 (2012) 23–29.
[35] C.-L. Yang, L.-Z. Wang, M.-S. Wang, X.-G. Ma, Quasi-classical trajectory study of the N(^{2}D) + H_2($X^1\Sigma_G^+$) → NH($X^3\Sigma^-$) + H(^{2}S) reaction based on an analytical potential energy surface, J. Phys. Chem. A 117 (2013) 3–8.
[36] D. Marx, J. Hutter, Ab Initio Molecular Dynamics: Basic Theory and Advance Methods, Cambridge University Press, New York, 2009.
[37] S.K. Gray, G.G. Balint-Kurti, Quantum dynamics with real wave packets, including application to three-dimensional (J = 0) D + H_2 → HD + H reactive scattering, J. Chem. Phys. 108 (1998) 950.
[38] Z. Sun, S.-Y. Lee, D.H. Zhang, A reactant-coordinate-based time-dependent wave packet method for triatomic state-to-state reaction dynamics: application to the H + O_2 reaction, J. Phys. Chem. A 113 (2009) 4145–4154.
[39] D.M. Neumark, A.M. Wodtke, G.N. Robinson, C.C. Hayden, K. Shobatake, R.K. Sparks, Molecular beam studies of the F + D_2 and F + HD reactions, J. Chem. Phys. 82 (1985) 3067.
[40] B. Fu, D.H. Zhang, A time-dependent quantum dynamical study of the H + HBr reaction, J. Phys. Chem. A 111 (2007) 9516–9521.
[41] D.H. Zhang, J.Z.H. Zhang, Accurate quantum calculation for the benchmark reaction H_2 + OH → H_2O + H in five-dimensional space: reaction probabilities for J = 0, J. Chem. Phys. 99 (1993) 5615.
[42] D.H. Zhang, J.Z.H. Zhang, Accurate quantum calculations for H_2 + OH → H_2O + H: reaction probabilities, cross sections, and rate constants, J. Chem. Phys. 100 (1994) 2697.
[43] Z.T. Cai, D.H. Zhang, J.Z.H. Zhang, Quantum dynamical studies for photodissociation of H_2O_2 at 248 and 266 nm, J. Chem. Phys. 100 (1994) 5631.
[44] R.N. Zare, Angular Momentum, Wiley, New York, 1988.
[45] D.M. Brink, G.R. Satchler, Angular Momentum, second ed., Clarendon, Oxford, 1968.
[46] P. Mcguire, D.J. Kouri, Quantum mechanical close coupling approach to molecular collisions. j_z-conserving coupled states approximation, J. Chem. Phys. 60 (1974) 2488.
[47] T. Gonzalez-Lezana, O. Roncero, P. Honvault, J.M. Launay, N. Bulut, F.J. Aoiz, L. Banares, A detailed quantum mechanical and quasiclassical trajectory study on the dynamics of the $H^+ + H_2 \rightarrow H_2 + H^+$ exchange reaction, J. Chem. Phys. 125 (2006) 094314.
[48] R.T. Pack, Space-fixed vs body-fixed axes in atom-diatomic molecule scattering. Sudden approximations, J. Chem. Phys. 60 (1974) 633.
[49] E.M. Goldfield, S.K. Gray, Adv. Chem. Phys. Illinois 60439, USA, 2007.
[50] R. Chen, H. Guo, The Chebyshev propagator for quantum systems, Comput. Phys. Commun. 119 (1999) 19–31.
[51] V.A. Mandelshtam, H.S. Taylor, A simple recursion polynomial expansion of the Green's function with absorbing boundary conditions. Application to the reactive scattering, J. Chem. Phys. 103 (1995) 2903.
[52] V.A. Mandelshtam, H.S. Taylor, Spectral projection approach to the quantum scattering calculations, J. Chem. Phys. 102 (1995) 7390.
[53] S.Y. Lin, H. Guo, Quantum state-to-state cross sections for atom-diatom reactions: a Chebyshev real wave-packet approach, Phys. Rev. A 74 (2006) 022703.
[54] G.G. Balint-Kurti, A.I. Gonzalez, E.M. Goldfield, S.K. Gray, Quantum reactive scattering of O(^{1}D) + H_2 and O(^{1}D) + HD, Faraday Discuss. 110 (1998) 169–183.
[55] N. Balakrishnan, C. Kalyanaraman, N. Sathyamurthy, Time-dependent quantum mechanical approach to reactive scattering and related processes, Phys. Rep. 280 (1997) 79–144.
[56] A.J. Meijer, E.M. Goldfield, S.K. Gray, G.G. Balint-Kurti, Flux analysis for calculating reaction probabilities with real wave packets, Chem. Phys. Lett. 293 (1998) 270–276.
[57] F.J. Aoiz, L. Banares, J.F. Castillo, Spin-orbit effects in quantum mechanical rate constant calculations for the F + H2 → HF + H reaction, J. Chem. Phys. 111 (1999) 4013.
[58] J. Zhang, S. Gao, Y. Song, Q. Neng, Int. J. Quantum Chem. 115 (2014) 231.
[59] H.S. Zhai, K.L. Han, New *ab initio* potential energy surface and quantum dynamics of the reaction H(^{2}S) + NH($X^3\Sigma^-$) → N(^{4}S) + H_2, J. Chem. Phys. 135 (2011) 104314.
[60] H. Umemoto, N. Hachiya, E. Matsunaga, A. Suda, M. Kawasaki, Rate constants for the deactivation of N(2^2D) by simple hydride and deuteride molecules, Chem. Phys. Lett. 296 (1998) 203–207.